View metadata, citation and similar papers at core.ac.uk

brought to you by CORE

provided by Kyoto University Research Information Repository

KURENAI 紅
Kyoto University Research Information Repository

KYOTO UNIVERSITY

Title	On the Buckling Strength of Angles in Transmission Towers
Author(s)	WAKABAYASHI, Minoru; NONAKA, Taijiro
Citation	Bulletin of the Disaster Prevention Research Institute (1965), 15(2): 1-18
Issue Date	1965-11-30
URL	http://hdl.handle.net/2433/124702
Right	
Type	Departmental Bulletin Paper
Textversion	publisher

Kyoto University

Bulletin of the Disaster Prevention Research Institute, Vol. 15, Part 2, No. 91, Nov., 1965

On the Buckling Strength of Angles in Transmission Towers

By Minoru WAKABAYASHI and Taijiro NONAKA

(Manuscript received September 30, 1965)

Abstract

It is assertained that buckling or instablility of angles has been the main cause of destruction of the super-structure of transmission towers due to typhoons. Experimental studies are made of buckling strength of angles, using structural steel with a L–90 mm× 90 mm×7 mm profile. Various eccentricities and slenderness-ratios are included. Behavior and modes of buckling failure are observed. Test results are compared with buckling theories, and a general consensus is reached between them. As an approach for safe and economical design of steel transmission towers, safety factors are examined for actual angle members based on the experimental results of the carrying capacity. Revision of JEC allowable stress is proposed.

Nomenclature

A	cross-sectional area
c	core radius
c_M	warping constant
E	Young's modulus
e	eccentricity
e_x	eccentricity in x-direction
e_y	eccentricity in y-direction
G	shear modulus
I_D	torsion constant
I_x	moment of inertia with respect to x-axis
I_y	moment of inertia with respect to y-axis
i_p	$\sqrt{\frac{I_x+I_y}{A}}$
i_M	$\sqrt{i^2{}_p+y^2{}_M}$
L	initial-curvature constant
l	length of angle
m	eccentricity ratio
n	eccentricity constant
P	compressive force
r	radius of gyration
r_{max}	maximum radius of gyration
r_{min}	minimum radius of gyration
r_x	$\frac{1}{I_x}\int_A y(x^2+y^2)dA$
t	thickness of leg
w	width of leg
x	coordinate along asymmetric principal axis of cross-section

y coordinate along symmetric principal axis of cross-section
y_M distance of shear center from x-axis
z coordinate along angle axis
λ effective slenderness ratio
λ_a ratio of actual length to minimum radius of gyration
σ axial stress
σ_c critical stress
σ_y yield point stress
φ torsional angle
φ_i initial torsional angle
τ ratio of tangent modulus to Young's modulus
μ Poisson's ratio
ν_a safety factor in actual condition
ν_i safety factor in ideal condition
ξ displacement of shear center in x-direction
η displacement of shear center in y-direction
Primes denote differentiation with respect to z.

Table of Contents pages

1. Damages of Transmission Towers due to Typhoon 2
2. Buckling Tests on Angles 4
(1) Scope of the tests 4
(2) Test specimen 5
(3) Loading equipment 5
(4) Deformation measurement 6
(5) Behavior and buckling mode 6
(6) Experimental results 7
(7) Buckling theories 7
(8) Comparison and discussion 10
3. Allowable Buckling Stresses 13
(1) Carrying capacity of tower angles 15
(2) Safety factors of tower angles 16
(3) Discussion of allowable stress 17
Summary 17
Acknowledgment 17
Bibliography 17

1. Damages of Transmission Towers due to Typhoon

It is often observed that transmission towers get damaged by typhoons, which almost regularly hit Japan. Reportedly, destructive typhoons take place once every few years somewhere in this country. In recent years, for example, Isewan Typhoon hit the middle part of Japan in 1959, and Muroto Typhoon II hit the western part in 1961, both having caused enormous damage to steel transmission towers. Among 13,563 towers, 63 were completely destroyed by Isewan Typhoon ; 66 were about to collapse ; 8 suffered some damage [1]* ;

* Numbers in square brackets refer to the Bibliography at the end of the paper.

hence, approximately one per cent of steel transmission towers got damaged in one way or another in this single typhoon.

In view of the fact that a great number of towers are constructed or repaired year after year, even a little saving of material is desirable in each tower member. In order to gain access to safety and economy requirements, we first have to know the causes or the mechanism of tower failures. Fig. 1 shows an example of collapsed transmission towers. It is not an easy task to find the direct cause for failures, but statistics show the

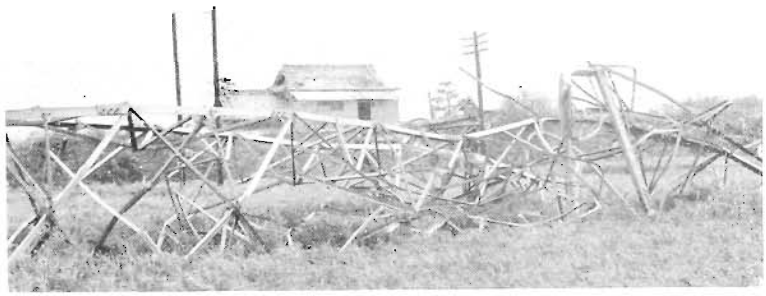

Fig. 1. Collapsed steel tower due to typhoon.

dominant cause is slipping of foundations from the ground. Either a foundation turns over or the post members slip through the foundation concrete. Improvement and minute care in the construction or design method are believed to greatly decrease these failures. What comes next, but not less important, is the failure in the superstructure. Most of failures in the super-structure are considered to be caused directly or indirectly by buckling of compression members. This is particularly true in large steel transmission towers [2]. Ishizaki, Ishida and Kawamura performed an experiment creating a model with the proto-type scale of a collapsed tower [3]. Fig. 2 is the picture of the tested tower model, which

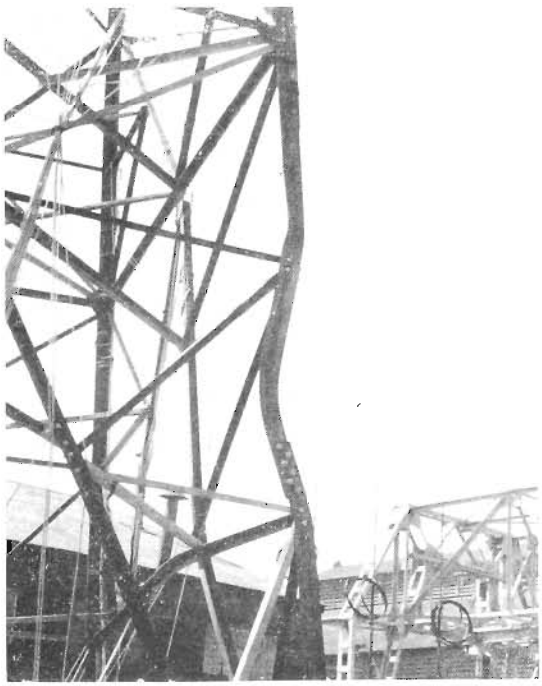

Fig. 2. Buckling failure of angle in steel tower.

indicates the importance of buckling phenomena in a compression member of a steel tower.

Design regulations of steel transmission toweres in this country are based on results of tower tests which have proto-type complications, and yet few experimental results seem to be available on buckling of a single member.

Among compression members of steel towers, most posts are subjected to nearly central thrust, and they are not so slender ; web members are mostly composed of an angle section, being connected at their legs to the main posts directly or through gusset plates. Hence, web members are apt to get eccentricity, and they are in addition often quite slender. Some constraints on the web members by posts have been considered to compensate the decrease in their buckling strength due to eccentricity, and for the design of a web member, it has been supposed to be simply supported at its ends. To rationalize the design method, however, the effects of the eccentricity and the constraints should be studied separately. Apart from the latter effect, we carried out some buckling tests and studied the behavior of angles under central and eccentric thrust.

2. Buckling Tests on Angles

(1) *Scope of the tests*

A total of fifty-seven specimens of mild steel angles L-90 mm×90 mm× 7 mm were tested and compared with buckling theories. The test program employed six kinds of eccentricity as shown in Fig. 3 (a). Solid circles show

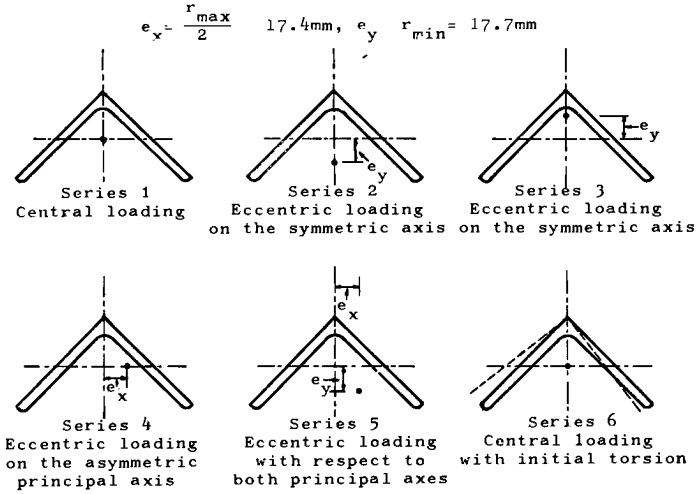

Fig. 3 (a). Eccentricities.

the points of load application. Series 1 is the central loading ; Series 2 and 3 are eccentric loading on the symmetric axis of the cross-section ; Series 4 on asymmetric principal axis. Series 5 has eccentricity with respect to both principal axes. Series 6 has initial torsion, and is subjected to central thrust. Amounts of eccentricities are also shown in the figure. r_{max} and r_{min} are

the maximum and minimum radii of gyration, respectively. Each series comprises the following values of the slenderness ratio (ratio of the angle length to the minimum radius of gyration) :

λ : 20, 40, 60, 70, 80, 90, 100, 110, 130, 150

with the exception of Series 6 (see Table 4).

(2) *Test specimen*

Specimens of each series have the same yield point stress σ_y as listed in Table 1. The material is called SS 41, having proved yield point stress 2,300 kg/cm^2 and ultimate stress somewhere between 4,100 and 5,000 kg/cm^2. The lengths of specimens are listed in Table 2. Fig. 3(b) shows the shape

TABLE 1.
Yield point stresses.

Series	1	2	3	4	5	6
σ_y (kg/mm^2)	31	33	33	32	32	30

TABLE 2.
Length of specimens.

λ	20	40	60	70	80	90	100	110	130	150
Length (cm)	34.5	70.8	106.2	123.9	141.6	159.3	177.0	194.7	230.1	265.5

of a specimen. Holes are made near the ends of the specimen to fix it on the supporting device. No heat treatment was made.

In Series 6, the initial torsion is distributed nearly uniformly along the column axis. In Table 3 are listed the relative twisting angles between ends.

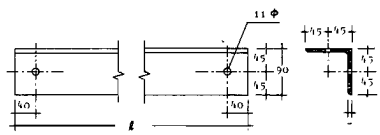

Fig. 3 (b). Specimen (unit:mm).

TABLE 3.
Relative twisting angles.

λ	20	40	60	70	80	90	100
Angle (degree)	0.52	0.55	0.81	1.87	1.65	1.22	1.52

(3) *Loading equipment*

Fig. 4 shows the end supports, which were designed to eliminate constraints against rotation and twisting at the specimen ends. Oil pressure is utilized for this purpose, oil being supplied to the upper and lower supports separately from a pump througth I, b, c and O, so that a thin oil membrance is formed between a and d. The center of rotation is located at the specimen end ; accordingly the buckling length equals the length l of a specimen. A support is equipped with screws and verniers for producing an exact eccentricity. Figs. 5 (a) and (b) are pictures of the end supports.

(4) Deformation measurement

Deflections and torsions were measured by dial gauges set as shown in Fig. 6.** Strains were also measured at various points by means of wire strain gauges. These measurements were made for observing the behavior of compressed angles.

(5) Behavior and buckling mode

(i) Series 1 (Central loading)

Long angles do not show appreciable deformation until the maximum loads are reached. They buckle relatively gradually in the direction of the symmetric axis of the cross-section. Angles with slenderness ratios between 70 and 100 buckle suddenly

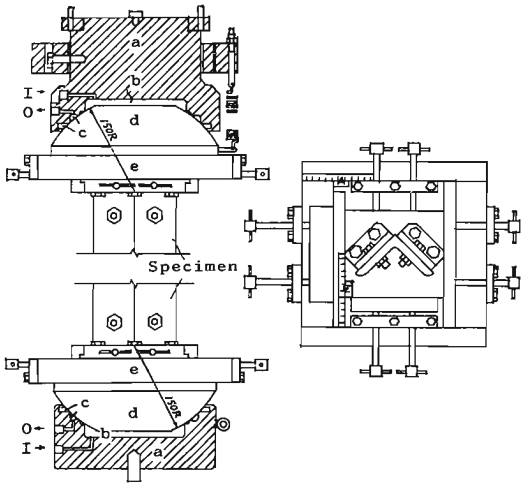

Fig. 4. End supports.

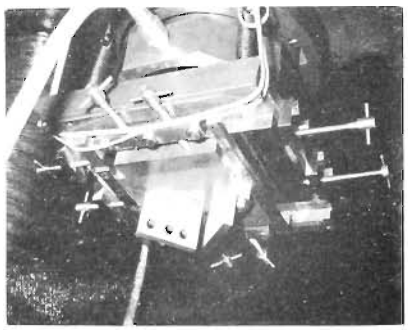

Fig. 5 (a). Upper support.

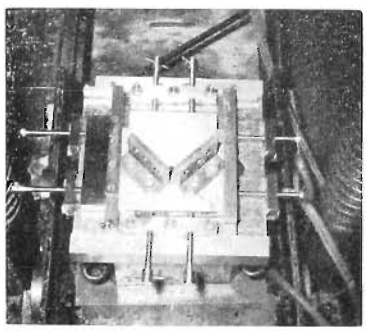

Fig. 5 (b). Lower support.

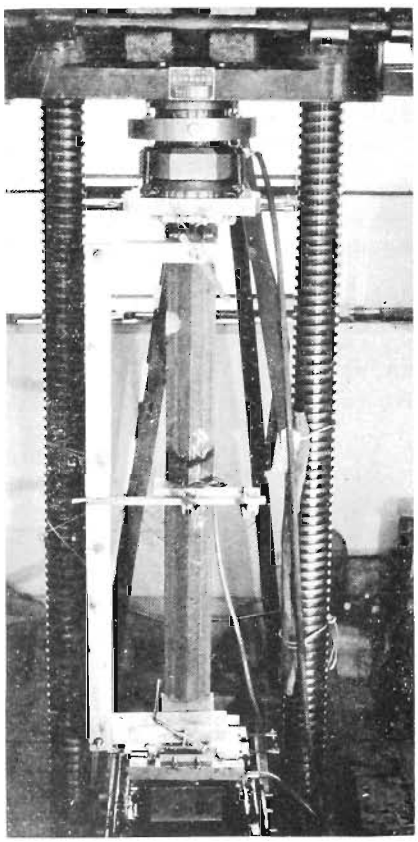

Fig. 6. Deformation measurement.

** Measurement device is described in detail in another paper [15].

under the buckling loads.*** Torsional deformation plays an important role in the buckling phenomena for short angles with slenderness ratio less than 70.

(ii) Series 2 (Eccentric loading on the symmetric axis)

Deflection increases steadily in the opposite direction to the eccentricity as the load increases.*** The cross-section does not change its shape until very large deflections are acquired after the maximum load is reached.

(iii) Series 3 (Eccentric loading on the symmetric axis)

Behavior is similar to Series 2 until the maximum load is reached. Since the eccentricity is given near the adjoing point of the legs, local buckling phenomena are not observed.

(iv) Series 4 (Eccentric loading on the asymmetric principal axis)

For small loads angles tend to deflect to the direction opposite to the eccentricity.*** As the loads approach the maximum loads their deflections increase rapidly in the most flexible direction, being accompanied by torsional deformation. Bending deformation dominates in long angles, but torsional or local deformation in short angles.

(v) Series 5 (Eccentric loading with respect to both principal axes)

Buckling phenomena take place quite slowly with increasing deflections and torsions as loads increase. Local buckling also happens in short angles.

(vi) Series 6 (Central loading with initial torsion)

Torsion increases steadily with the load. Bending deformation resembles that in Series 1.

(6) *Experimental results*

Buckling stresses and collapse modes are listed in Table 4. Measured maximum loads are taken as the buckling loads. Cross-sectional area has been measured for each specimen. In the table, B stands for bending, TB for torsional flexural and L for local buckling.

(7) *Buckling theories*

TABLE 4.
Buckling stresses and modes.

Slenderness ratio	Buckling stresses (kg/cm²)						Buckling modes					
	Series						Series					
	1	2	3	4	5	6	1	2	3	4	5	6
20	2,960	1,638	1,932	1,907	1,417	2,860	TB	B	B	L	L	L
40	2,960	1,446	1,561	1,832	1,183	2,850	TB	B	B	L	L	TB
60	2,873	1,219	1,342	1,740	1,046	2,815	B	B	B	B	B	TB
70	2,923	1,121	1,252	1,638	953	2,644	TB	B	B	B	B	B
80	2 644	1,055	1,160	1,696	892	2,719	B	B	B	B	B	B
90	2,338	966	1,041	1,731	828	2,295	B	B	B	TB	B	B
100	2,208	884	977	1,591	813	1,980	B	B	B	B	B	B
110	1,913	809	867	1,623	777		B	B	B	B	B	
130	1,327	667	738	1,282	680		B	B	B	B	B	
150	1,000	580	619	968	552		B	B	B	B	B	

*** See Blbliography 15.

Let x and y be the coordinate axes along the principal axes of the angle cross-section as shown in Fig. 7. z-axis is taken along the column axis.

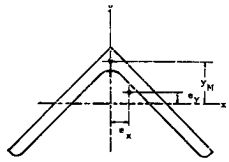

Fig. 7.

(i) Flexural buckling

Under the central thrust, bending about x-axis occurs independently, unless local buckling takes place, and the buckling stress σ_c is given in the elastic range from Euler's theory

$$\sigma_c=\frac{\pi^2 E}{\lambda^2} \tag{1}$$

where E is the Young's modulus. For inelastic buckling, the tangent modulus theory gives

$$\sigma_c=\frac{\pi^2 \tau E}{\lambda^2} \tag{2}$$

where τ is the ratio of tangent modulus to Young's modulus. According to DIN 4114 [4], τ can be approximated as

$$\tau=1-\left(\frac{\sigma-\sigma_p}{\sigma_y-\sigma_p}\right)^2 \tag{3}$$

for stress σ such that $\sigma_p \leqq \sigma \leqq \sigma_y$, and $\sigma_p \cong 0.8\sigma_y$ where σ_p is the proportional limit and σ_y is the yield stress.

(iii) Local buckling

Since an angle is composed of plate elements, i. e., two legs, it is possible that, before the inception of instability due to integral failure of the column, the legs reach a state of unstable equilibrium and buckle locally. In case of an equal angle under central thrust, the local buckling can be approximately analysed as for a plate element which has dimensions of a leg of the angle and is simply supported along three edges with the other edge free as shown in Fig. 8. With notations given in the figure, and with Poisson's ratio μ, the critical stress for such a plate is given by Bleich [5] as

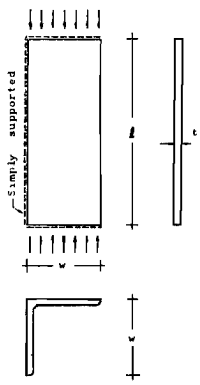

Fig. 8.

$$\sigma_c=\frac{\pi^2 E\sqrt{\tau}}{12(1-\mu^2)}\left(\frac{t}{w}\right)^2\left(0.425+\frac{w^2}{l^2}\sqrt{\tau}\right) \tag{4}$$

When the length of the angle is very long compared with the width of its legs, this is approximated as

$$\sigma_c=0.425\frac{\pi^2 E\sqrt{\tau}}{12(1-\mu^2)}\left(\frac{t}{w}\right)^2 \tag{5}$$

(iii) Torsional flexural buckling

Assuming the shape of the cross-section does not change due to buckling, Kollbrunner and Meister [6] give the equilibrium relation in the elastic range for slightly bent angles under eccentric thrust P as

$$\left.\begin{aligned}&EI_y\xi''''+P\xi''+P(y_M-e_y)\varphi''=0\\&EI_x\eta''''+P\eta''+Pe_x\varphi''=0\\&EC_M\varphi''''+\{P(i_P^2+y_M^2)-GI_D+Pe_y(r_x-2y_M)\}\varphi''\\&\qquad+P(y_M-e_y)\xi''+Pe_x\eta''=0\end{aligned}\right\}\tag{6}$$

where ξ, η : displacements of the shear center in x- and y-directions
e_x, e_y : eccentricities in x- and y-directions
φ : torsional angle
I_x, I_y : moments of inertia of the cross-section with respect to x- and y-axes
I_D : torsion constant
G : shear modulus
C_M : warping constant with respect to shear center
y_M : distance of shear center from x-axis

$$i_P^2\equiv\frac{I_x+I_y}{A}$$

$$i_M^2\equiv i_P^2+y_M^2$$

$$r_x\equiv\frac{1}{I_x}\int_A y(x^2+y^2)dA$$

A : cross-sectional area

and primes denote differentiation with respect to z.

If we use boundary conditions that at $z=0$ and l

$$\xi=\eta=\varphi=\xi''=\eta''=\varphi''=0\tag{7}$$

then the critical stress for elastic torsional flexural buckling is given as the smallest root of the following equation:

$$\begin{aligned}&(\sigma_x-\sigma_c)(\sigma_y-\sigma_c)\left\{\sigma_t-\sigma_c-\sigma_c\frac{e_y(r_x-2y_M)}{i_M^2}\right\}\\&\qquad-\sigma_c^2(\sigma_x-\sigma_c)\frac{(y_M-e_y)^2}{i_M^2}-\sigma_c^2(\sigma_y-\sigma_c)\frac{e_x^2}{i_M^2}=0\end{aligned}\tag{8}$$

where

$$\left.\begin{aligned}&\sigma_x\equiv\frac{\pi^2EI_x}{Al^2}\\&\sigma_y\equiv\frac{\pi^2EI_y}{Al^2}\\&\sigma_t\equiv\frac{1}{Ai_M^2}\left(GI_D+\frac{\pi^2EC_M}{l^2}\right)\end{aligned}\right|\tag{9}$$

It is recalled that $\lambda=\dfrac{l}{r_{min}}$ and that $r_{min}^2=\dfrac{I_x}{A}$.

For central loading, $e_x=e_y=0$ and tangent modulus theory allows Eq. (8) to be used for inelastic range also, provided E and G are multiplied by τ, or equivalently

$$\left(\sigma_x-\frac{\sigma_c}{\tau}\right)\left\{\left(\sigma_y-\frac{\sigma_c}{\tau}\right)\left(\sigma_t-\frac{\sigma_c}{\tau}\right)-\left(\frac{\sigma_c}{\tau}\right)^2\frac{y_M^2}{i_M^2}\right\}=0.\tag{10}$$

Bleich [7] has shown that for an equal angle under central thrust the torsional flexural buckling theory and the local buckling theory give approximately equal value of the critical stress. Clearly, Series 1 and 6 correspond to the condition that $e_x=e_y=0$; Series 2 and 3 $e_x=0$, $e_y\neq 0$; Series 4 $e_x\neq 0$, $e_y=0$; Series 5 $e_x\neq 0$, $e_y\neq 0$.

In case of the experiment reported herein, the boundary conditions are such that the displacements, bending moments, twisting moments and warpings vanish at both ends, but the difference in the solutions between these boundary conditions and Eq. (7) is found to be small [8][9]; Eq. (7) gives much simpler solution. For these reasons, we use above solutions in the present paper.

(iv) Ježek's theory

The torsional flexural buckling theory does not hold in inelastic range for eccentric loading. It is noted that in Series 2 and 3 the carrying capacity is controlled by bending in the symmetric plane of an angle An approximate analysis is presented for inelastic bending in such a case by Ježek [10]. Assuming elastic-perfectly plastic behavior of the material, we can approximately determine the maximum stress σ_c from

$$\lambda^2=\frac{\pi^2 E}{\sigma_c}\left\{\frac{3\left(\frac{\sigma_y}{\sigma_c}-1\right)-m}{3\left(\frac{\sigma_y}{\sigma_c}-1\right)}\right\}^3 \qquad \text{if} \quad \lambda^2\geqq\frac{\pi^2 E m^3}{9\sigma_y(3-m)} \tag{11}$$

and

$$\lambda^2=\frac{\pi^2 E}{\sigma_y}\sqrt{\frac{\sigma_c}{\sigma_y}\left(\frac{\sigma_y}{\sigma_c}-\frac{\sigma_c}{\sigma_y}-\frac{2}{3}m\right)^3} \qquad \text{if} \quad \lambda^2<\frac{\pi^2 E m^3}{9\sigma_y(3-m)} \tag{12}$$

where m is the ratio of the eccentricity e_y to the core radius in the compressive side. Eq. (11) is valid when yielding occurs only in the compressive side and Eq. (12) when yielding occurs both in the tensile and compressive sides.

(v) Modified local buckling theory

When an angle is subjected to eccentric compression on the asymmetric principal axis, as in Series 4, the instability may primarily be induced by local buckling of leg OE (Fig. 9), which is compressed more strongly than the other leg. C is the point of loading. We approximately reckon that the critical load is the one that produces the critical stress given by Eq. (5) on that leg when the load is distributed uniformly on each leg, the intensity being inversely proportional to the distances $\overline{BC}$ and $\overline{CA}$. This idea shall later be called modified local buckling theory.

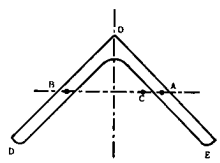

Fig. 9.

(vi) Buckling of initially twisted angles

When the column is twisted initially by amount $\varphi_i(z)$, then the equilibrium equations in (6) must be modified so that the first and third equations of (6) include the terms $-Py_M\varphi_i''$ and $-Pi_M^2\varphi_i''$, respectively, in the left hand side. When φ_i is a linear function of z, as in Series 6, these terms vanish, and hence the equilibrium equations coincide with those for straight angles.

(8) *Comparison and discussion*

Experimental results and the predictions from the above buckling theories are compared in Figs. 10-14. In Fig. 14 the ordinate is proportional to the critical stress, and the abscissa to the slenderness ratio, both being dimensionless.

(i) Series 1

Fig. 10 shows that the experiment has close agreement with Euler's theory, Eq. (1) for long columns, with tangent modulus theory, Eq. (2) for me-

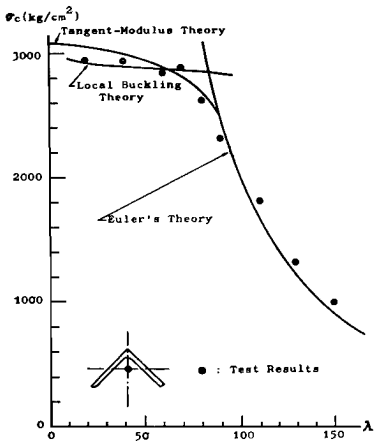

Fig. 10. Series 1.

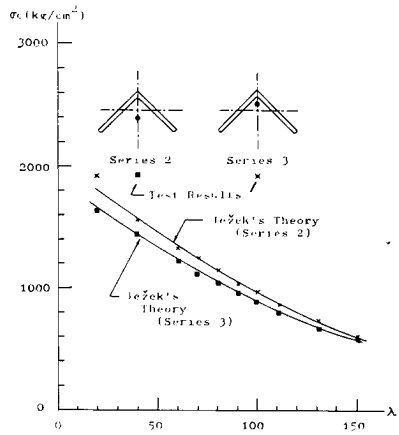

Fig. 11. Series 2 and 3.

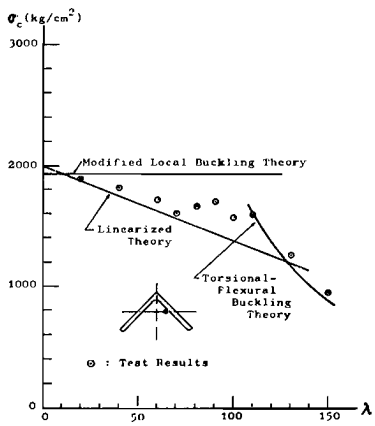

Fig. 12. Series 4.

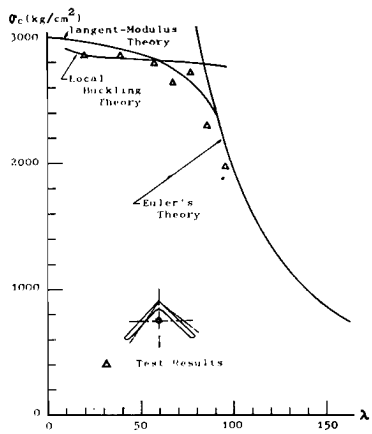

Fig. 13. Series 6.

dium lengths, and with the torsional flexural buckling theory, Eq. (10) or the local buckling theory of plate elements, Eq. (4) for short columns. It was observed during the experiment that angles with λ less than 62 buckled due to torsion combined with bending, exactly as the torsional flexural buckling theory predicts.

(ii) Series 2 and 3

General agreement is seen between the experiment and Ježek's theory in

Fig. 11.

(iii) Series 4

Straight line labelled as linearized theory in Fig. 12 is obtained by connecting the point corresponding to the elastic limit strength by short column theory, with zero length, to the point correponding to the state where the elastic limit stress is reached somewhere in the column according to torsional flexural buckling theory, Eq. (8). We see that the experimental results agree with the torsional flexural buckling theory for long angles, and they lie for

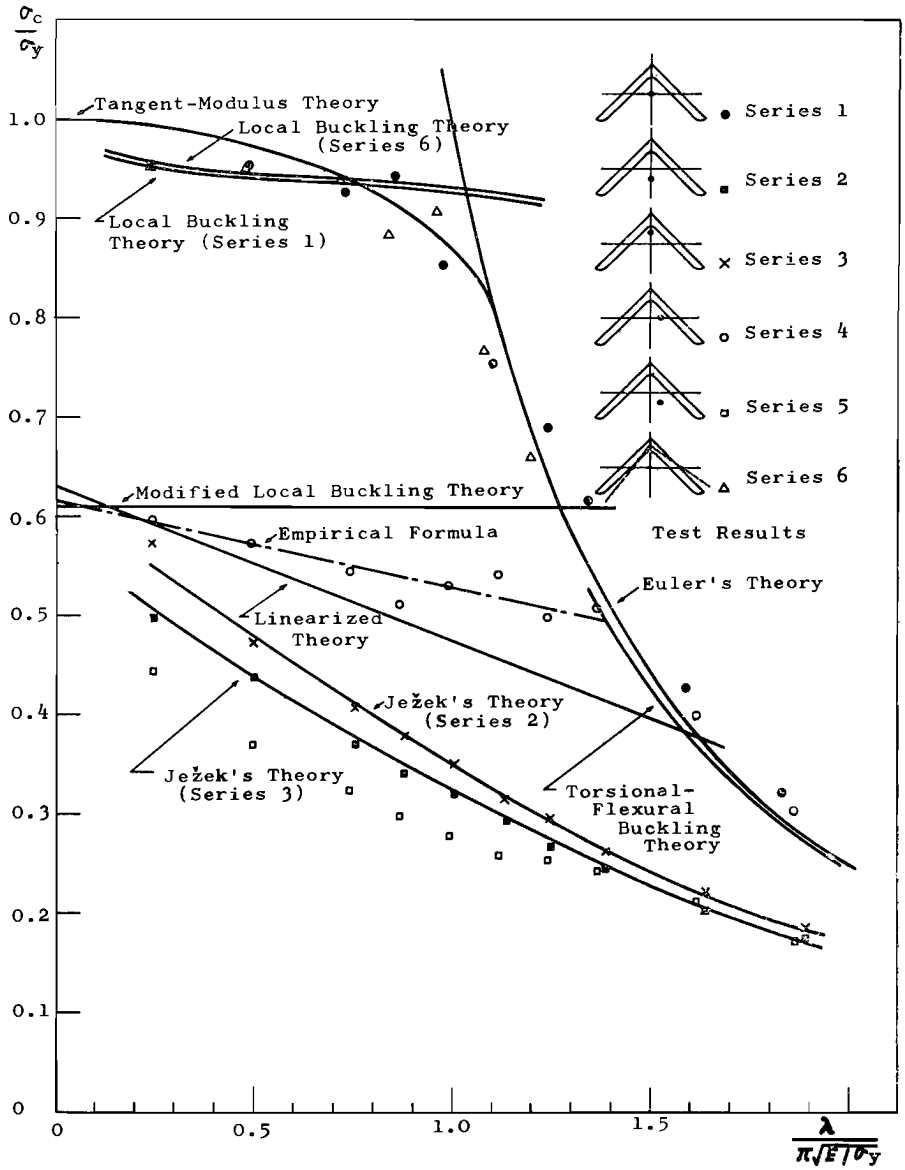

Fig. 14. Comparison among series.

inelastic range between the predictions from the modified local buckling theory and the linearlized theory.

(iv) Series 6

As mentioned already, theories predict the same critical stresses for Series 6 and 1. This is confirmed in the experiment as is seen in Figs. 13 and 14.

(v) Comparison among series

In Fig. 14 are compared all test results. Theoretical curves are included in the figure. An empirical formula is also added with a chain line for short and medium lengths in Series 4, obtained from the method of least squares.

It is seen both experimentally and theoretically that the buckling strength or the carrying capacity is decreased by eccentricities, and that Series 5, which has eccentricities with respect to both principal axes, has the smallest critical stresses. There is some difference in the effects of eccentricities on the symmetric axis and on the asymmetric principal axis. The eccentricity on the symmetric axis reduces the capacity for all angles. This is concerned with bending deformation; bending occurs by considerable amount due to the eccentricity before the maximum load is reached, because of small flexural rigity for bending in the plane of symmetry, and this is well taken care of by applying, e.g., Ježek's theory. On the other hand, when we compare the theoretical and experimental results for Series 1 with those for series 4, we see that the decrease in the capacity due to the eccentricity on the asymmetric principal axis is not appreciable for long angles (for eccentricity of the amount given here). This is also seen when we compare the test results for Series 2 and 5. The decrease for short angles is primarily caused by local buckling or torsional deformation, but the carrying capacity of long angles is primarily concerned with bending in the most flexible direction, i.e., in the symmeric plane.

3. Allowable Buckling Stresses

We will now examine the allowable buckling stresses based on the experimental and theoretical results presented in the previous section.

In this country, steel transmission towers are designed in accordance with JEC [11]. JEC does not distinguish the allowable buckling stresses between main posts and web members. In Fig. 15 is compared the JEC allowable stress**** with the allowable stresses in foreign countries [12]. We see that the Japanese code gives a relatively high allowable stress as compared with other countries. Fig. 16 shows the safety factors which allowable buckling stresses of these provisions possess, calculated on the basis of the tangent modulus theory. The figure indicates relatively small safety factor of the Japanese code, particularly for large slenderness ratios. The reason for this is considered to be that the experimental results on which JEC provisions are based were

---

**** JEC-127 gives the allowable buckling stress σ_a(kg/cm^2) for SS41 as

$$\sigma_a=\begin{cases}1{,}450-500(l/100r)^2 & \text{for} \quad 0\leqq l/r\leqq 100\\ 1{,}900\div\{1+(l/100r)^2\} & \text{for} \quad 100\leqq l/r\leqq 220\end{cases}$$

where the length l is taken to be the distance between the end joints, and r the minimum radius of gyration of the cross section. Since 1953, the allowable unit stress is specified to be 1,450 kg/cm^2 for tension, compression and bending.

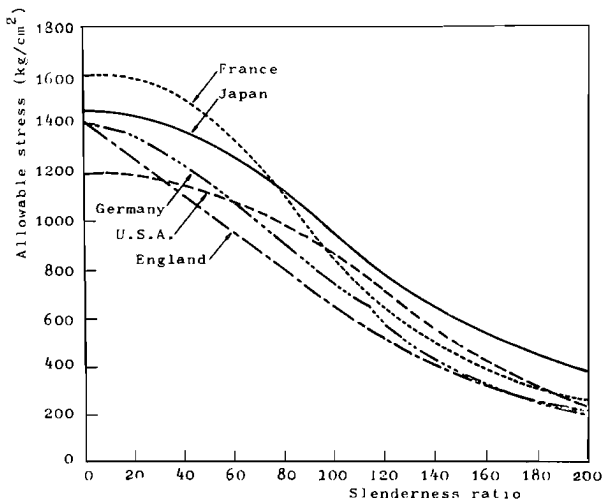

Fig. 15. Comparison of allowable stresses (for SS41 equivalent material).

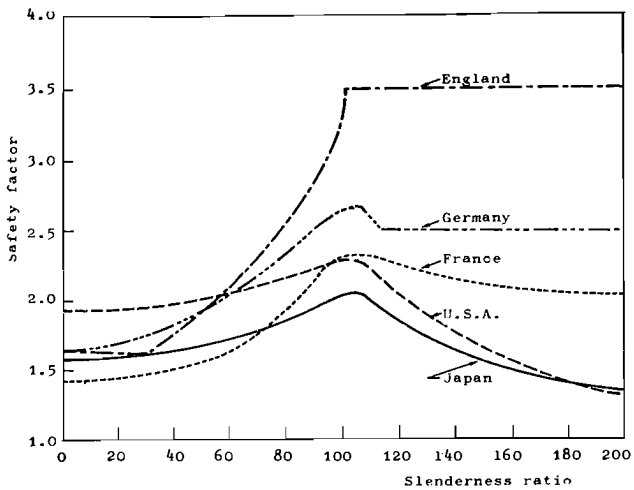

Fig. 16. Safety factors of allowable stresses against tangent-modulus critcial stress.

obtained in proto-type model tests or tests in which there were some end constraints for column members under consideration. Slenderness ratios were, therefore, overestimated in these tests. In an actual steel tower slender angles, which are often used as web members, are provided with some end constrains through main posts. On the other hand, they are mostly subjected to eccentric thrust, and the weakening effect due to eccentricity should also be taken into account.

Apart from the effects of end constraints, we will first examine the carrying capacity of compressed angles in actual condition, and then estimate the safety factors of angles under working compressive stresses against the carrying capacity. It is desirable to design a steel tower so that all structural

members bear the same safety factor.

(*1*) *Carrying capacity of tower angles*

As pointed out in the first section, post and web members are essentially in different conditions in a steel tower. In order to determine the carrying capacity of a compressed angle, both cases of central and eccentric compression must be clarified.

(i) Central loading

From studies in the previous section, we have found that the buckling stress is given from:

a) Euler's theory, Eq. (1) for long angles,

b) tangent modulus theory, Eq. (2) for medium lengths, and

c) local buckling theory of plate elements, Eq. (4) (or torsional flexural buckling theory, Eq. (10)) for short angles.

(ii) Eccentric loading

Some eccentricity is inevitable in angle members of a steel tower even with the greatest possible care in the construction. Furthermore, under normal conditions an angle has some initial deflection. Both of these effects reduce the carrying capacity of a compressed angle. The former may primarily depend on the size of the cross-section and the latter on the length of an angle. We approximately regard these effects as being produced by an eccentricity e composed of two terms, one of which is proportional to the radius of gyration r and the other to the length l, i.e.,

$$e=\frac{r}{n}+\frac{l}{L} \tag{13}$$

where constant n depends on the eccentricity of loading and L on the initial curvature, both being dimensionless and independent of the cross-section and the length.

The ratio m of the ecentricity e to the core radius c in the compressive side is

$$m=\frac{r}{c}\left(\frac{1}{n}+\frac{\lambda}{L}\right) \tag{14}$$

The constant r/c in Eq. (14) depends only on the shape of the cross-section.

By examining actual angles which are often used in transmission towers in this country, these constants are evaluated as shown in Table 5.

TABLE 5.
Eccentricity constants

Constants		Measured values	Approximation
$\frac{r}{c}$		1.95 ~ 2.14	2
n	post	11.2 ~ 39.7	20
	web	3.2 ~ 6.6	5
L		1,000 ~13,000	1,000

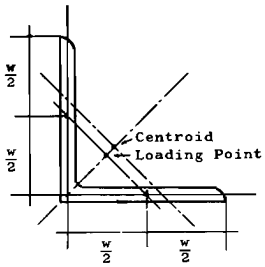

Fig. 17. Post member.

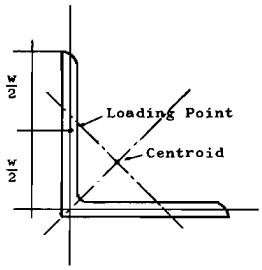

Fig. 18. Web member.

These constants refer to the eccentricity on the symmetric axis of the cross-section. Due to connection mechanisms, post members generally have a little eccentricity on the symmetric axis as in Fig. 17, and web members have eccentricity with respect to both principal axes as in Fig. 18. The eccentricity on the symmetric axis can well be taken care of by applying Ježek's theory, Eqs. (11) and (12). Although the eccentricity in the direction of the asymmetric principal axis, in web members, also reduces the carrying capacity, studies in the previous section have shown that the reduction is not serious for long angles. For short angles, this eccentricity induces considerable torsional deformation, and reduces, the carrying capacity appreciably. Reviewing the experimental results for Series 4, we estimate the maximum stress of short web members as sixty percent of the yield stress.

(2) *Safety factors of tower angles*

Based on the carrying capacities thus calculated, safety factors of the allowable stress of JEC provision have been evaluated for SS41 and are shown graphically in Fig. 19. In the abscissa is taken the ratio λ_a (apparent slenderness ratio) of the actual length of an angle to the minimum radius of gyration. The solid line shows the safety factor with respect to the carrying capacity for central loading, the chain line to post members, and the dotted line to web members.

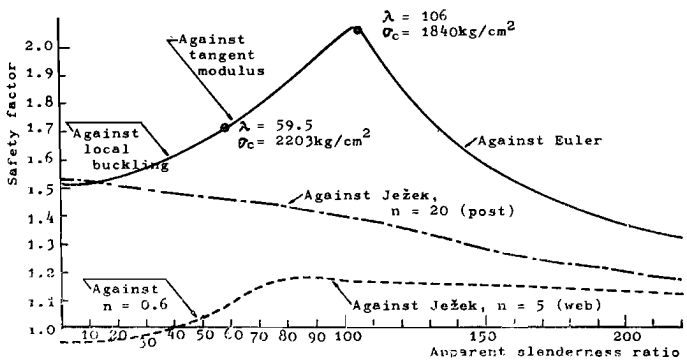

Fig. 19. Safety factor of JEC allowable stress (SS41).

It should be noted that the JEC allowable stress bears different values of the safety factor ν_a for post and web members in actual conditions. In the figure

also included is the safety factor ν_i (solid line) which the allowable stress would possess if an angle were subjected ideally to central thrust. We see that ν_i is maximum at $\lambda_a=106$, and that $\nu_i<1.5$ for $\lambda_a>165$. For post members ν_a steadily decreases as λ_a increases, and $\nu_a<1.3$ for $\lambda_a>140$. For web members, ν_a is quite small, and what is most noticeable is that $\nu_a<1$ for $\lambda_a<40$.

(3) *Discussion of allowable stress*

Let us propose to design angles for compression so that in any case, say, $\nu_i \geqq 1.5$ and $\nu_a \geqq 1.3$. Since much end constraints cannot be expected for post members, they should be designed so that $\lambda_a<150$, when subjected to compressive forces. Since web members generally have some end constraints, their carrying capacities for long angles may be somewhat higher than the values evaluated in the above (equivalently, the effective slenderness ratio is decreased). According to experimental data [13] and theoretical estimation [14], the increase of the carrying capacity due to the end constraints can be expected to be more than 20% for $\lambda_a>80$. Consequently, the condition that $\nu_i \geqq 1.5$ and $\nu_a \geqq 1.3$ is found to be satisfied for web members with λ_a between 80 and 220. However, small value of ν_a for $\lambda_a<80$ is due mainly to the reduction in the carrying owing to the eccentricity in the direction of asymmetric principal axis, and the end constraints cannot be expected to compensate this reduction. Hence, the allowable stress should be reduced for web angles under compression with $\lambda_a<80$. Revision of JEC code has thus been proposed for the allowable buckling stresses of angle members.

Summary

On the assertion that buckling of angles is one of main causes of the failure of transmission towers due to typhoon, some series of buckling tests have been made. A total of fifty-seven specimens were tested, using L-90×90×7 of SS41. It was observed that various types of buckling caused the failure of angles under longitudinal compression, according to eccentricity and angle dimensions. Bending, torsion and Beulung (local buckling of plate elements) play an important role in the buckling strength of angles. A general agreement was seen between the experiment and buckling theories. Safety factors of JEC allowable buckling stress were examined, based on the experimental results of the carrying capacity. Revision of the JEC provision has been proposed such that in steel transmission towers upper-bound of slenderness ratio of compressed angles should be specified for post members and that the allowable buckling stress should be lowered for short web members.

Acknowledgment

The results presented in this paper were obtained in the course of research sponsored by Yawata Iron and Steel Co., Ltd. under the supervision of Dr. Y. Yokoo, Professor of Nagoya University. The authors wish to thank Mr. A. Ishida of Japan Bridge Co. for his cooperation in the discussion of the last section.

Bibliography

1. Investigation Committee on Damages due to Isewan Typhoon, "Reports on Damages

due to Isewan Typhoon", Architectural Institute of Japan, Tokyo, 1961, pp. 125–126 (In Japanese).
2. op. cit. in Bibliography 1, pp. 129–131.
3. H. Ishizaki, A. Ishida and S. Kawamura, "On the Full-Sized Model Test of Transmission Tower Destroyed by a Typhoon (Part 1, Static Loading Test), Transactions of the Architectural Institute of Japan, No. 81, January, 1963, pp. 22–27 (In Japanese).
4. Deutsche Industrie-Norm, Code Number 4114. See, e.g., "Stahl im Hochbau", Verlag Stahleisen M. B. H., Düsseldorf, 1953, p. 165 (In German).
5. F. and H. Bleich, "Buckling Strength of Metal Structures", McGraw-Hill Book Co., New York, 1952, p. 327.
6. C. F. Kollbrunner and M. Meister, "Knicken, Biegedrillknicken, Kippen", Second Edition, Springer-Verlag, Berlin, 1961, p. 157 (In German).
7. op. cit. in Bibliography 5, p. 135.
8. Y. Yokoo, M. Wakabayashi and T. Nonaka, "Experimental Studies on Buckling Strength of Angles (Part 1, Preliminary Tests)", Transactions of the Architectural Institute of Japan, No. 69, October, 1961 (In Japanese) ; and
T. Nonaka, "Studies on the Problem of Buckling in Steel Structures", Thesis for the Degree of Master of Science, Kyoto University, 1961, pp. 10–13.
9. N. Ueda, "Effects of Boundary Conditions on the Buckling Strength of Torsion and Flexure", Thesis for the Degree of Bachelor of Science, Kyoto University, 1962 (In Japanese).
10. op. cit. in Bibliography 5, pp. 34–40.
11. JEC (Japan Electric Code) 127 (in Japanese).
12. op. cit. in Bibliography 6, pp. 279–292.
13. A. Ishida and N. Kawamura, "Experimental Study on the Effective Buckling Length of Web Members in a Tower", Transactions of the Architectural Institute of Japan, Extra Summaries of Technical Papers of Annual Meeting of A. I. J., 1965, p. 304 (In Japanese).
14. Op. cit. in Bibliography 9.
15. M. Wakabayashi and T. Nonaka, "Experimental Study on Buckling Behavior of Angles", Annual of the Disaster Prevention Research Institute, Kyoto University, No. 9, to be published in March, 1966 (In Japanese with English captions).